Progress Towards a Global Digital Elevation Model for Mercury

Kris J. Becker[1], Tammy L. Becker[1], Kenneth L. Edmundson[1], Robert W. Gaskell[2], Ralph L. McNutt, Jr.[3], Scott L. Murchie[3], Gregory A. Neumann[4], Mark E. Perry[3], Louise M. Prockter[3], Mark S. Robinson[5], Sean C. Solomon[6,7], Grant K. Stephens[3], F. Scott Turner[3], and Lynn A. Weller[1]

[1]Astrogeology Science Center, United States Geological Survey, Flagstaff, AZ 86001; [2]Planetary Science Institute, 1700 East Fort Lowell, Suite 106, Tucson, AZ 85719; [3]Johns Hopkins University Applied Physics Laboratory, Laurel, MD 20723; [4]NASA Goddard Space Flight Center, Greenbelt, MD 20771; [5]School of Earth and Space Exploration, Arizona State University Tempe, AZ, 85287; [6]Lamont-Doherty Earth Observatory, Columbia University, Palisades, NY 10964; [7]Department of Terrestrial Magnetism, Carnegie Institution of Washington, Washington, DC 20015
(kbecker@usgs.gov)

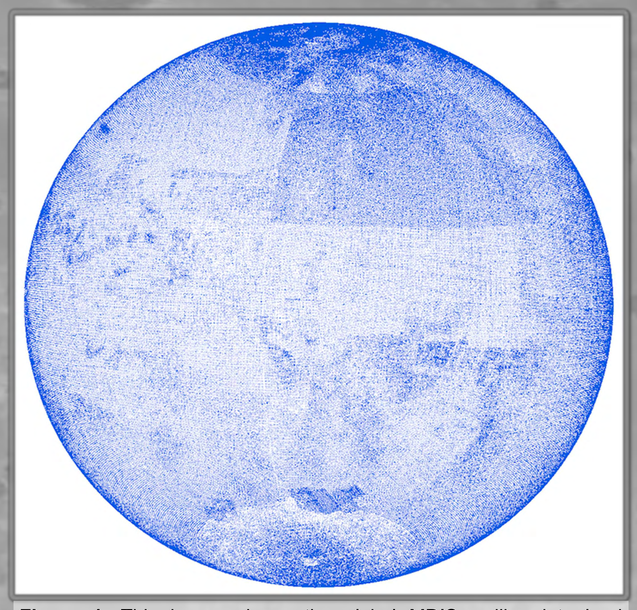

Figure 1. This image shows the global MDIS radii point cloud generated from the USGS control network in Mercury body fixed coordinates. North is at the top.

Control Network: The USGS is developing a global control point network, continuously adding MDIS images as they are acquired [4]. The current control network point cloud (**Figure 1**) was created from 60,281 MDIS NAC and WAC-G filter images acquired from April 5, 2011 through June 11, 2013. The network contains a total of 555,120 ground points. A least squares bundle adjustment was applied to the network to improve image pointing and orientation. As shown in **Table 1**, spatial RMS accuracy is near a quarter of a pixel and 100 meters in radius.

Modified Shepard's Equation

Eq. 1

$$w_i = \frac{\left[\frac{R-h_i}{Rh_i}\right]^2}{\sum_{j=1}^{n}\left[\frac{R-h_j}{Rh_j}\right]^2}$$

where h_i is the distance from the interpolation point to control point i; R is the distance from the interpolation point to the most distant control point; n is the total number control points in that interpolation point

Eq. 2

$$\emptyset = \sum_{i=1}^{n} \emptyset_i w_i$$

where $\emptyset_i$ is the radius value at each control point; w_i is the inverse distance weight from Eq. 1; n is the total number of control points in the map point

Figure 3. Equations for the inverse distance weighted function how it is applied to the point could radii to compute the interpolated output map data number. **Eq. 1** shows the weight applied to each control point radius resulting from the kd-tree search in **Eq. 2** for each map grid point.

Introduction: For nearly three years now, the Mercury Dual Imaging System (MDIS) narrow-angle camera (NAC) and multispectral wide-angle camera (WAC) [1] on the Mercury Surface, Space ENvironment, GEochemistry, and Ranging (MESSENGER) spacecraft [2] acquired more than 200,000 images of Mercury's surface. These data enable creation of a digital elevation model (DEM) of Mercury for eventual release through the Planetary Data System (PDS). Data acquired by the Mercury Laser Altimeter (MLA) combined with radio occultation data provide a comparison model, summarized in [3], for the MDIS DEM. We present an update on the status toward our goal of a global topographic shape model for general use in research and analysis of Mercury's surface.

Bundle Adjustment	
images	60,281
angle constraints	±0.2°
ground points	555,120
all points constrained in radius	±10 km
line/sample measurements	6,599,703

image space	root mean squared error of line/sample residuals (pixels)		
	sample	line	All residuals
Bundle adjustment	0.21	0.26	0.24

object space	root mean squared error of triangulated ground point coordinate uncertainties (meters)		
	latitude	longitude	radius
Bundle adjustment	32	55	98

Table 1. Summary of least squares bundle adjustment results of MDIS control point network.

References: [1] Solomon S. C. et al. (2001) *Planet. Space Sci.*, *49*, 1445-1465. [2] Hawkins S. E. III. et al. (2007) *Space Sci. Rev., 131,* 247-338. [3] Becker K. J. et al. (2014) LPSC 45, abs #2243. [4] Becker K. J. et al. (2012), LPSC 43, abs #2654. [5] Franke R., Nelson G., (1980) *Numerical Methods in Engineering*, 15, 1691-104. [6] Neumann G. A. et al. (2013) *Science*, 339, 296-300. [7] Chabot N. S. et al. (2012) *Geophys. Res. Lett.*, doi:10.1029/2012GL051526.

Future work: Additional research will be conducted to determine the best possible interpolation method for sparsely populated point clouds. We will be making similar comparisons with the DEM to the MLA and radio occultation standard topographic model to assess improvements to NAC and WAC camera models and development techniques. A final global DEM product will be produced with an appropriate resolution to be released to the PDS.

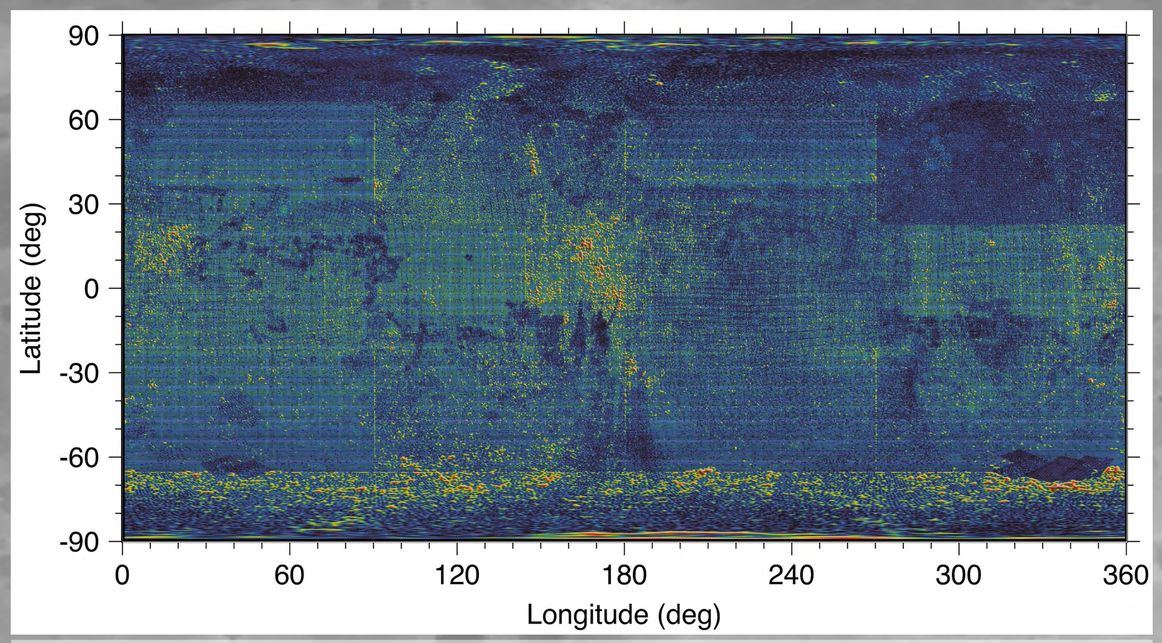

Figure 2. Equirectangular projection at 1 km/pixel showing the minimum distance in kilometers at each map grid point center to a network control point (see **Fig. 1**). Green/yellow areas correspond to control points that are farthest away from map point centers. Blue/dark blue are closest.

Point Cloud Analysis: Due to limitations in illumination, resolution and stereo coverage, point density varies in the control network. Specialized software using kd-trees was developed to analyze the control point cloud. A 1 km/pixel sinusoidal equal-area map was used to analyze how the radius control points populate each pixel in the map. The point cloud populates approximately 1.7 million km^2 of the 74.8 million km^2 surface area of Mercury or 2.28%. 95.93% of those map points contain only one control point and 3.69% contain two points. The remaining map points contain three or more control points (6,359 km^2) most likely located in the polar regions. **Figure 2** shows the distribution of the closest distance to a point in the control network from the center of each map grid. The closets points are within 5 cm of the center of a grid point with the maximum distance being near 45.7 km. The average distance is 5.65 km with a standard deviation of 2.8 km. A DEM map product created at 5 km/pixel would be populated by ~50% of the control points.

DEM Generation: Radius values at each map grid point are calculated using a modified Shepard's inverse distance weighted function [5]. The point cloud kd-tree is searched first using a radial search of 1.4142 km (distance from geodetic center to grid point corner). If no points are found to be within the radial search range, a neighbor search of 5 points is used. The interpolation equation in **Figure 3** was used to produce the DEM shown in **Figure 4**. There exists an inherent lack of control points in both poles due to permanently shadowed areas [6,7]. Improvements in topography were made in nearly every area in comparison with the previously created MDIS standard as seen in **Figure 5**. The average radius of the DEM is 2439.83 km.

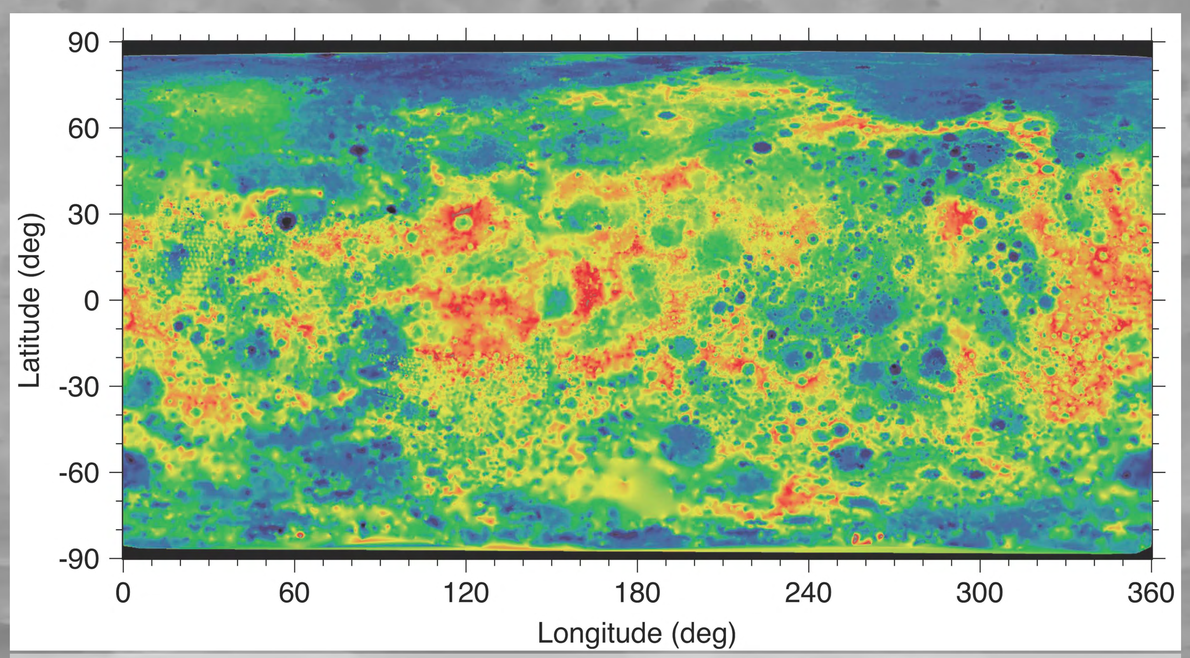

Figure 5. Global equirectangular DEM map rendered at 1 km/pixel produced from the control point network as summarized in [4]. The network contains 263,762 points, 24,507 images and 1,857,334 measures. Comparisons of this DEM to the combined MLA and radio occultation DEM product have established the baseline topographic standard for Mercury.

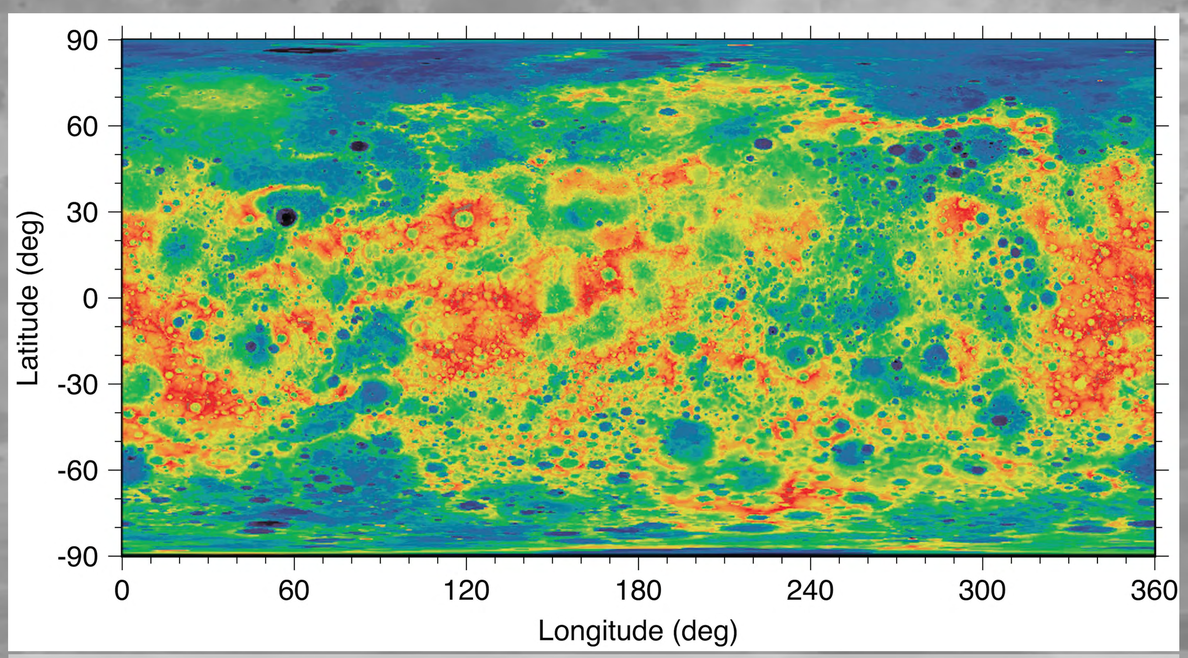

Figure 4. Interpolation in **Fig. 3** was applied to the global control point network from **Fig. 1** to produce this 1 km/pixel equirectangular DEM. **Fig. 5** is provided for comparison of improvements that have been made since the last report in [4]. Most areas have increased topographic detail and accuracy from improvements to the MDIS camera thermal models and increased density in the point cloud.